Mechanical and Sensitivity Analysis of 43.5 mm bore Nb_3Sn Dipole Model

D. R. Chichili and G. Ambrosio
Technical Division
Fermilab, Batavia, IL 60510

1.0 INTRODUCTION

Various designs for the mechanical support structure were evaluated and reported in a previous technical note TD-99-030. The two final designs chosen for further consideration are discussed here. Both these designs have aluminum spacers with clamp and skin acting as structural elements. In the first design the pre-stress in the coils is obtained through the interference between the clamp and the yoke and weld shrinkage. Further there is azimuthal interference between the spacer and the pole extension to avoid excessive loading at room temperature. In the second design there is no interference between the yoke and the clamp and between spacer and the pole extension; instead the pre-stress is obtained through gradually varying radial interference between the spacer and the yoke and as well as due to weld shrinkage. Note that in both the designs the yoke gap remains open at all stages of the magnet.

This report presents the mechanical and sensitivity analysis for the 43.5 mm bore Nb_3Sn dipole model. It was decided that we would go with the clamp/yoke interference design for the first dipole model. The reader is referred to TD-99-030 for material properties and the magnet mechanics for the two designs mentioned above.

2.0 43.5 mm Bore Dipole Design Parameters

Table 1 summarizes the general features of the design. The primary difference between the 44.5 and 43.5 mm bore designs is that the insulation thickness went up from 5 mils to 10 mils. To accommodate this and to maintain the same outer diameter as in 44.5 mm bore design (in order to use the LHC IR Quard tooling), the inner radius was decreased accordingly.

Parameter	Unit	44.5 mm design	43.5 mm design
Cable insulation thickness	mm	0.125	0.25
Number of turns		54	48
Total coil area	mm^2	2512	2233
B_{ss}	T	12.28	12.02
I_{ss}	A	18139	19574
Stored energy @11T	kJ/m	252	241
Pole width	mm	16.36	15.09

Table 1: *Design parameters for 44.5 and 43.5 mm bore designs [TD-99-027].*

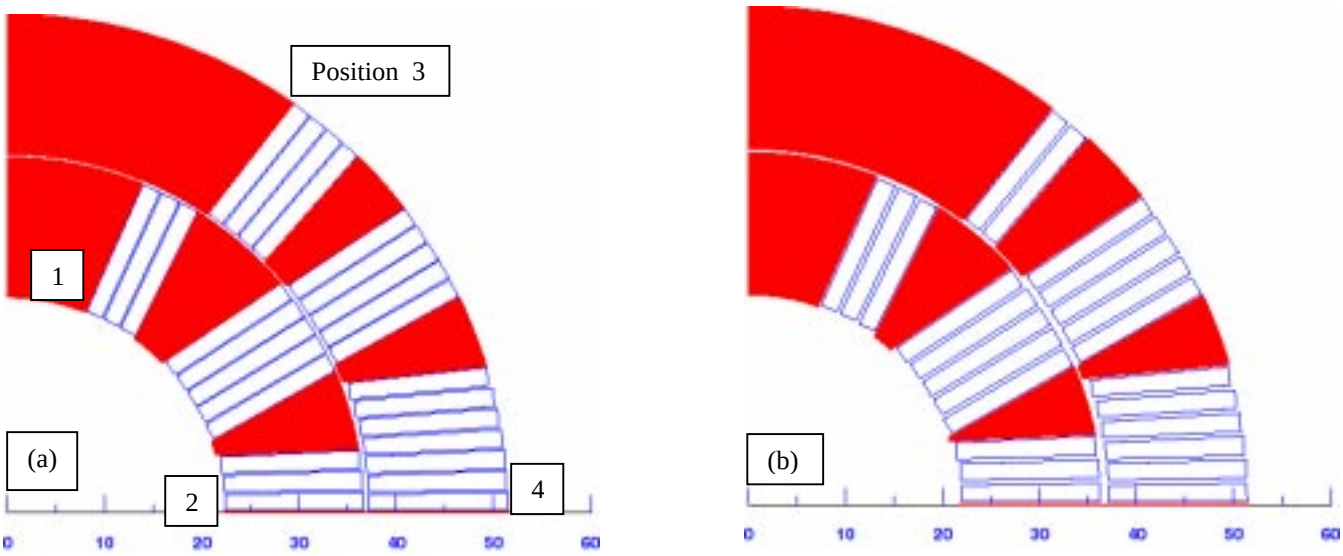

Figure 1: *Cable and wedge layout for (a) 44.5 mm bore design and (b) 43.5 mm bore design [from TD-99-027].*

Fig. 1 shows the cable and wedge layout for the two designs. The number of turns in the outer layer has also been reduced from 16 to 13 per quadrant. However the inner layer is same for both the designs. Since the total number of turns have been decreased, the critical current density, I_{ss} increased from 18139 A to 19574 A.

Block	Comp	Unit	43.5 mm design	44.5 mm design
1	F_r	KN/m	197	241
	F_θ	KN/m	-241	-274
2	F_r	KN/m	113	126
	F_θ	KN/m	-503	-456
3	F_r	KN/m	32	80
	F_θ	KN/m	-290	-551
4	F_r	KN/m	473	463
	F_θ	KN/m	-109	-99
5	F_r	KN/m	631	635
	F_θ	KN/m	-614	-556
6	F_r	KN/m	170	186
	F_θ	KN/m	-579	-556
ANSYS Total	F_r	KN/m	1616	1731
	F_θ	KN/m	-2336	-2492
	F_x	KN/m	2812	3024
	F_y	KN/m	-1057	-1101
ROXIE Total	F_x	KN/m	2812	3025
	F_y	KN/m	-1062	-1103

Table 2: *Magnetic forces at quench field on each block and total force computed by ANSYS and ROXIE.*

2.0 Magnetic Analysis

The characteristics of the magnetic analysis can be found in TD-99-031. Here we report a comparison between the 43.5 and the 44.5 mm bore design. Table 2 lists the magnetic forces at quench field on each coil block and the total force on a quadrant. The total force computed by ROXIE is also reported. Note that the center field for 44.5 mm bore design is 12.28 T and for 43.5 mm bore design is 12.02 T. In Figs. 2 and 3 the magnetic forces at quench field on each element of the coils for 44.5 and 43.5 mm bore design are presented.

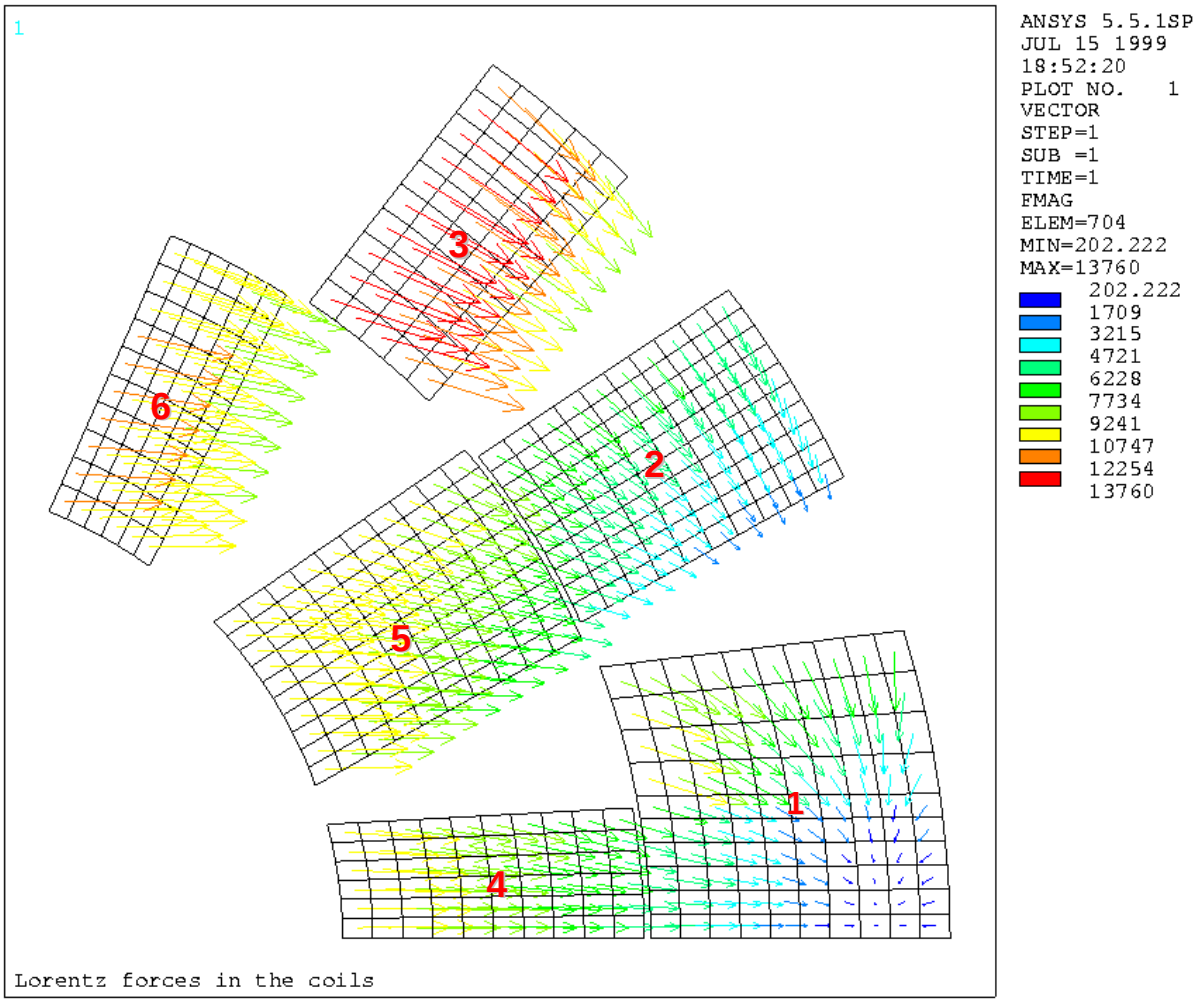

Figure 2: *Lorentz forces in the cross-section of 44.5 mm bore design.*

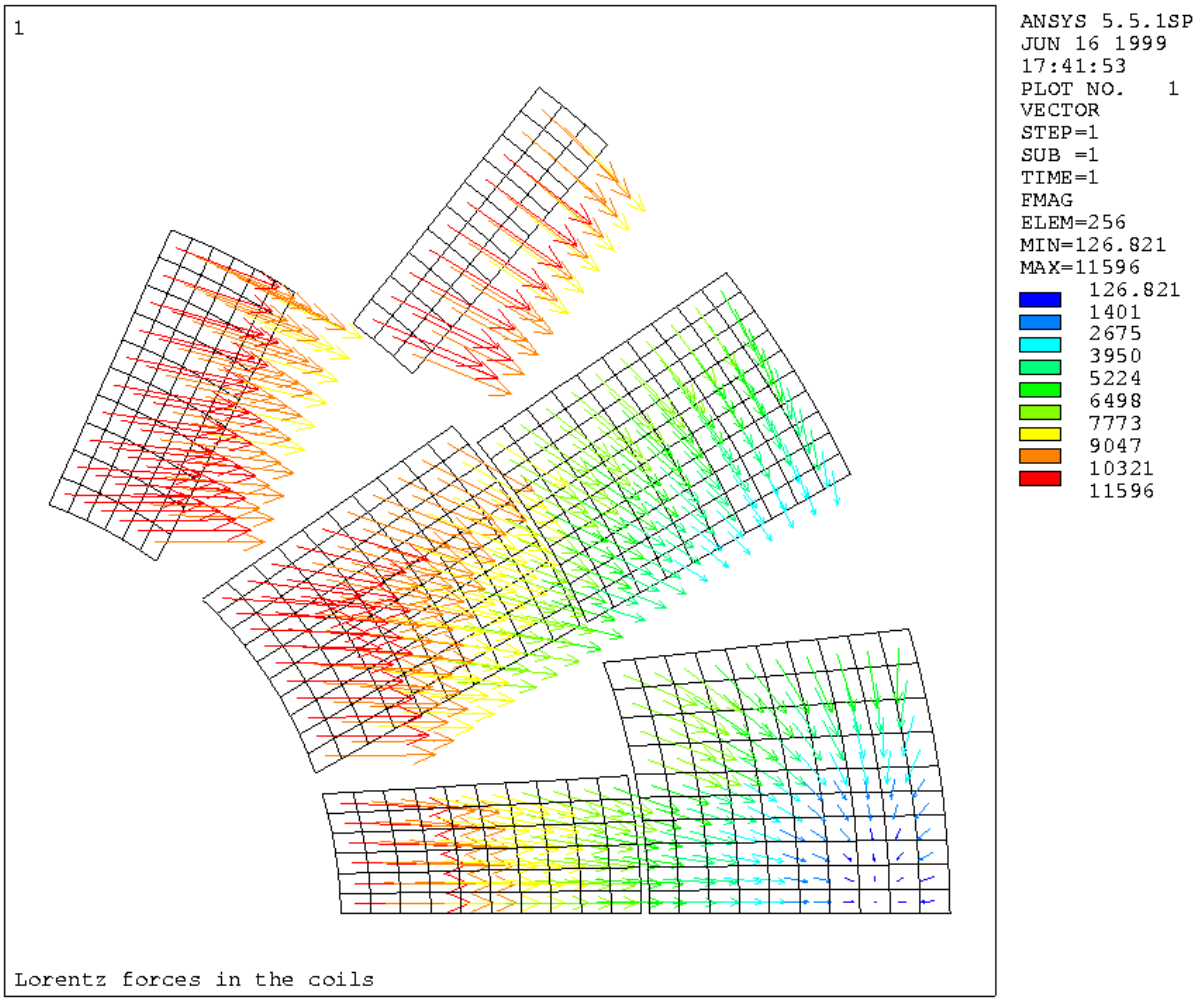

Figure 3: *Lorentz forces in the cross-section of 43.5 mm bore design.*

4.0 Mechanical Analysis of the Nominal Design

For the same amount of clamp/yoke and spacer/pole interference, Table 3 summarizes the pre-stress distribution for 43.5 and 44.5 mm bore magnet designs [clamp/yoke interference = 0.35 mm, spacer/pole interference = 0.15 mm, weld shrinkage = 0.4 mm]. Note that the inner coil at Position-1 lost all the pre-stress for 43.5 mm design, where as for 44.5 mm design, the coil is still under compression. This is due to the fact that the former design has higher Lorentz forces in the inner coil than the later design (see Fig. 1 for locations of the positions in the coil assembly).

To achieve enough pre-stress for 43.5 mm bore design, the yoke/clamp interference was increased to 0.4. This increases the peak stress to 112 MPa after cool down and the coil assembly remains under compression up to 11 T. However, Position - 1 of the coil assembly sees tension at 12.08 T. Figs. 4 and 5 show the stress distribution in the coils and in the spacer. Note that the

spacer is under compression and is in contact with the coil assembly and the yoke at all stages of the magnet. The displacement contour plot for the coil assembly is shown in the Fig. 6. The aperture at the mid-plane and at the pole remains the same at all conditions except during cool-down.

	44.5 mm Design Stress, MPa				**43.5 mm Design** Stress, MPa			
	300 K	**4.2 K**	**11 T**	**12 T**	**300 K**	**4.2 K**	**11 T**	**12 T**
COIL								
Position 1	67	116	11	2 / -12	68	107	**-1.36**	
Position 2	83	26	90	97	81	23	104	
Position 3	62	78	33	42	63	88	57	
Position 4	67	100	100	97	68	107	104	

Table 3: *Comparison of the pre-stress in the coil assembly for 44.5 and 43.5 mm designs.*

	Azimuthal Stress, MPa				**Radial Stress, MPa**			
	300 K	**4.2 K**	**11 T**	**12 T**	**300 K**	**4.2 K**	**11 T**	**12 T**
COIL								
Position 1	74	112	16 / 4	-6	0	4	-1	-2.5
Position 2	90	32	100	102	0	4	-1	-2.5
Position 3	70	94	67	62	38	42	38	29
Position 4	74	112	111	116	44	54	88	94
SPACER	233	200	166	166				
σ_{coil}(max)	93	111	101	113	=Von-mises stress			
CLAMP	176	170	174	174	=Von-mises stress			
SKIN	220	303	330	340	=Von-mises stress			
δR	3	-81	0	30	=R(mid-Plane)-R (pole); μm			

Table 4: *Stresses in the various components of the magnet for optimized interferences.*

Note that the above analysis was carried out with a cut in the pole. This was simulated my merely removing the boundary conditions in that region. However in the real magnet, the cut will be machined out in the pole region and filled with some insulating material and then impregnated with epoxy with the rest of the coil assembly. So to accurately model this process, we need to create an additional area in the pole with some filler material.

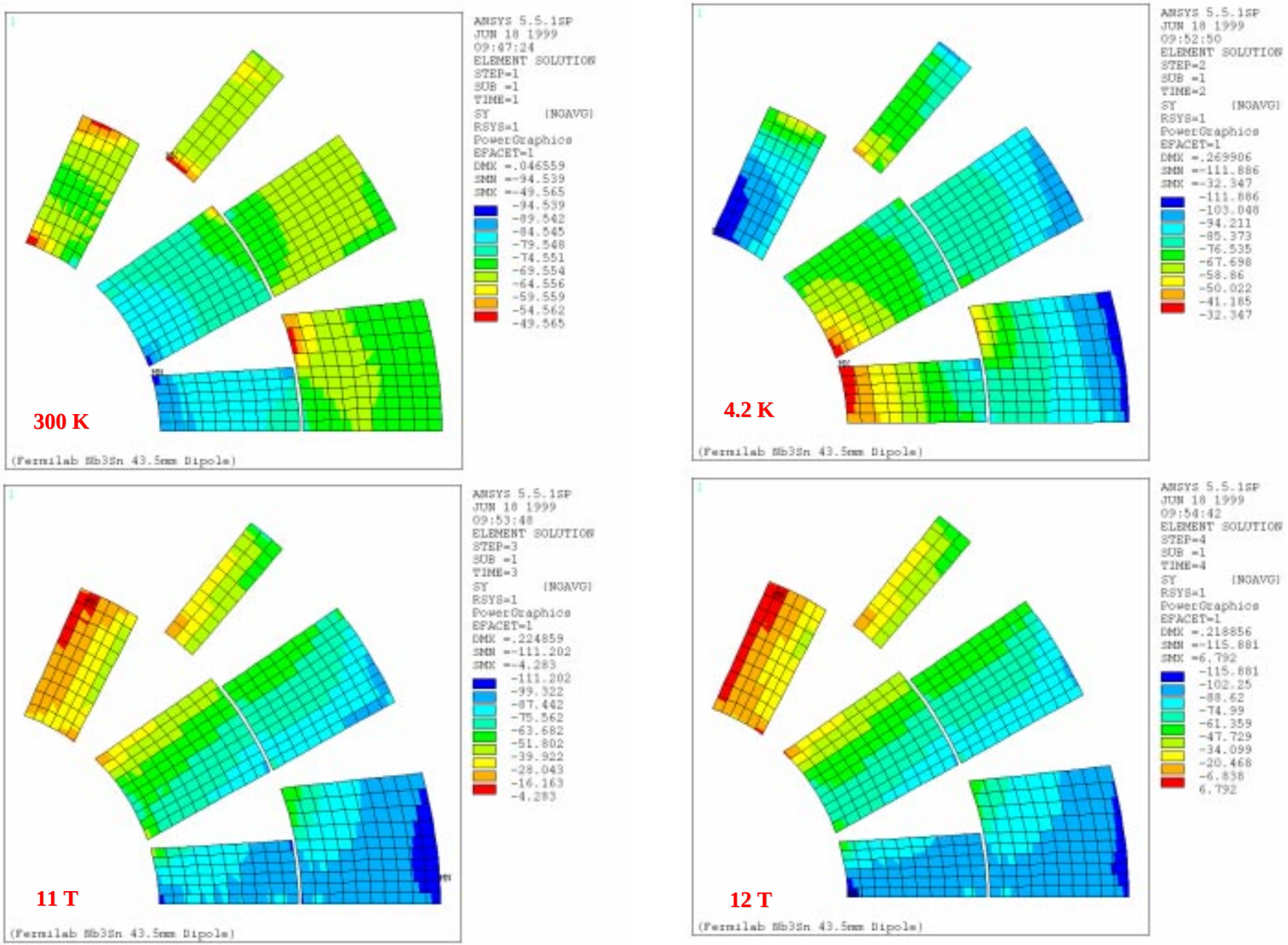

Figure 4: *Azimuthal stress distribution in the coil assembly*.

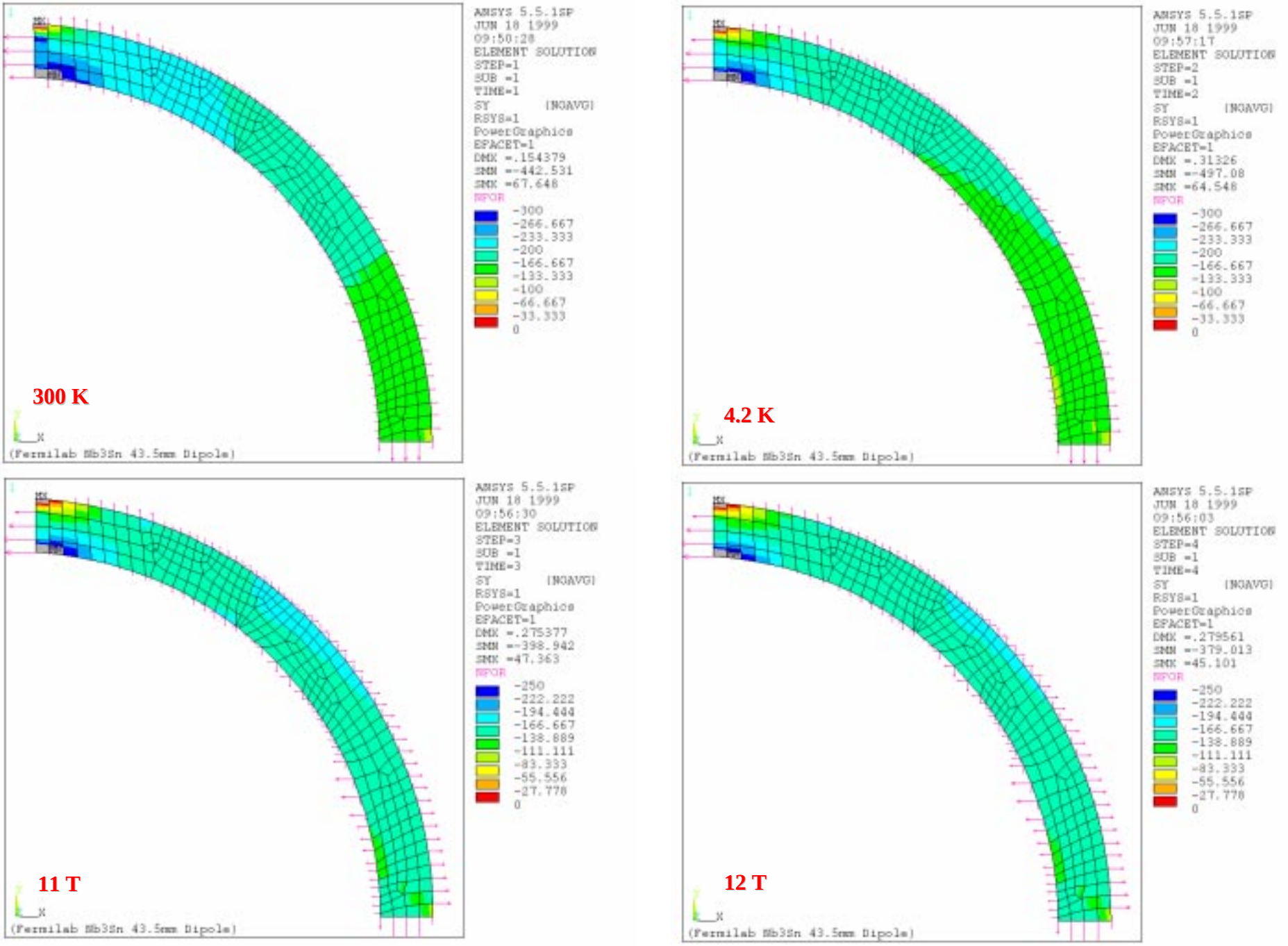

Figure 5: *Azimuthal stress distribution in the aluminum spacer*.

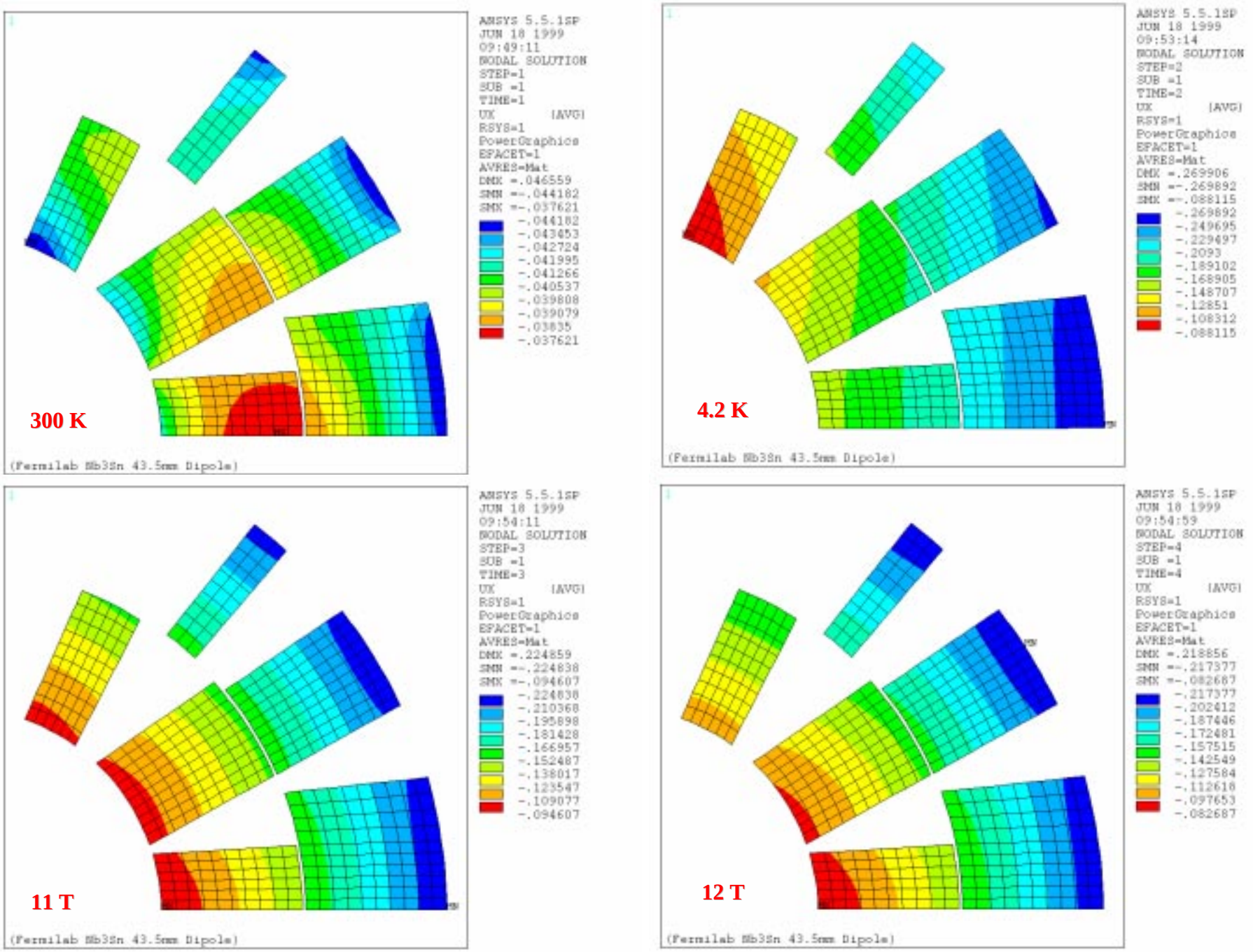

Figure 6: *Displacement contour plots of the coil assembly.*

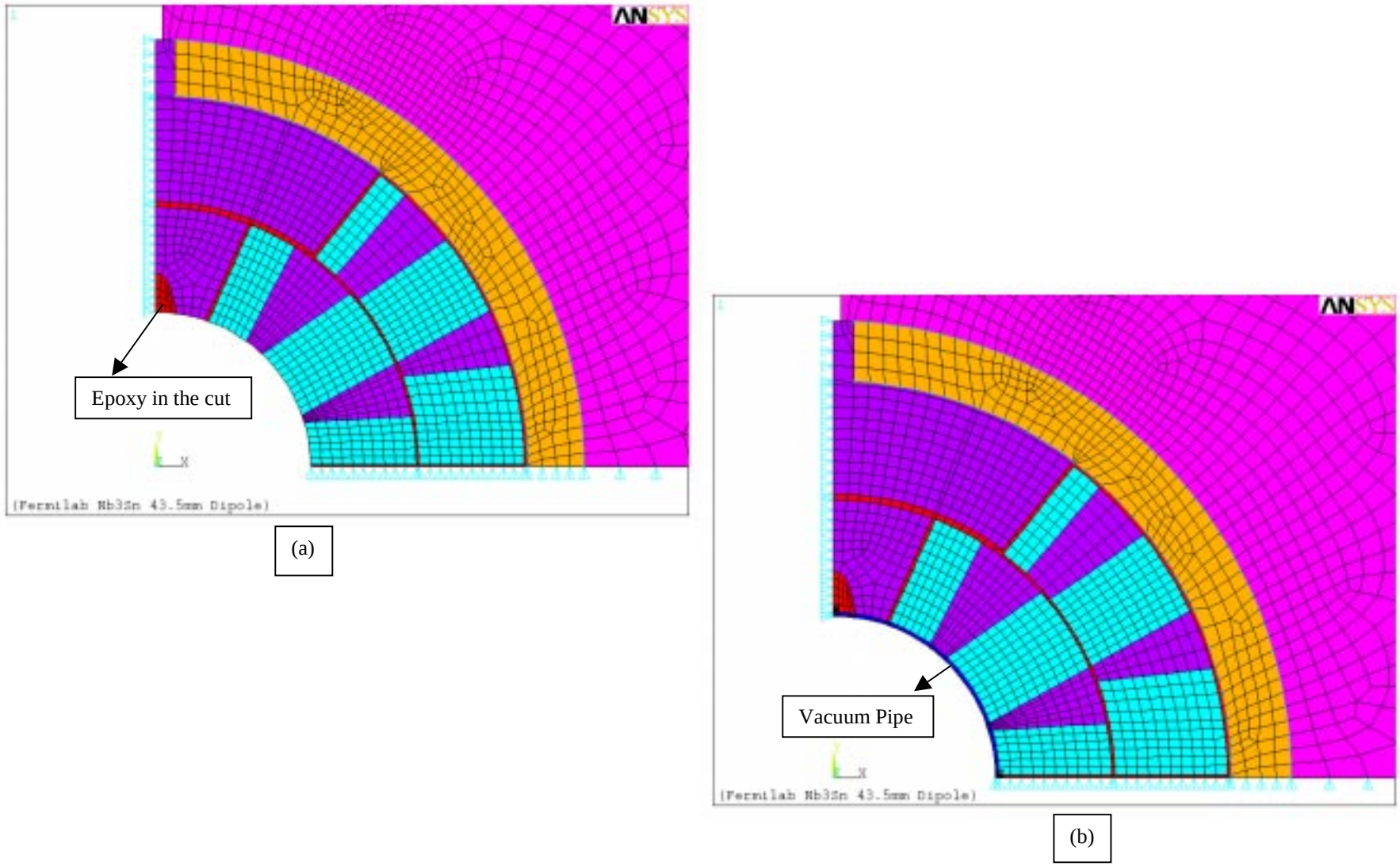

Figure 7: *Model with (a) epoxy in the pole cut with no vacuum pipe; (b) epoxy in the pole cut with vacuum pipe.*

4.1 Model with Filler Material in the Pole Cut

Fig. 7(a) shows the model used to analyze the epoxy in the pole cut due to vacuum impregnation. The properties of this material were considered to be same as G-10. For the same parameters used in the previous simulation i.e., yoke/clamp interference = 0.4 mm; spacer/pole interference = 0.15 mm and weld shrinkage = 0.4 mm, Table 5 lists the stresses in the various components of the magnet.

	Azimuthal Stress, MPa				Radial Stress, MPa			
	300 K	**4.2 K**	**11 T**	**12 T**	**300 K**	**4.2 K**	**11 T**	**12 T**
COIL								
Position 1	74	114	7	-11	1.6	0	-4	-6
Position 2	90	32	100	101	1.6	0	-4	4
Position 3	63	95	65	60	37	44	40	40
Position 4	74	105	111	115	42	57	81	97
SPACER	233	200	152	152	50	60	85	90
σ_{coil}(max)	93	114	101	111	=Von-mises stress			
CLAMP	206	200	202	200	=Von-mises stress			
SKIN	226	304	340	330	=Von-mises stress			
δR	3.6	-81	0	30	=R(mid-Plane)-R (pole); μm			

Table 5: *Stresses in the various components of the magnet with epoxy in the pole cut, without vacuum pipe.*

	Azimuthal Stress, MPa				Radial Stress, MPa			
	300 K	**4.2 K**	**11 T**	**12 T**	**300 K**	**4.2 K**	**11 T**	**12 T**
COIL								
Position 1	67	96	12	-14	3	8	-5	-6
Position 2	83	32	73	81	8	8	26	27
Position 3	63	87	61	54	45	46	37	39
Position 4	71	105	109	109	50	58	90	95
SPACER	216	200	152	512	50	62	87	91
σ_{coil}(max)	80	100	100	101	=Von-mises stress			
VP	475	700	500	500	=Von-mises stress; Vacuum pipe			
CLAMP	206	204	200	204	=Von-mises stress			
SKIN	227	308	340	340	=Von-mises stress			
δR	3	-81	0	30	=R(mid-Plane)-R (pole); μm			

Table 6: *Stresses in the various components of the magnet with epoxy in the pole cut and with vacuum pipe.*

The peak stress in the coils with epoxy in the pole cut is about 115 MPa (see Appendix for the stress distribution in the coils). The stress distribution in the coils especially after cool down was found to be quite sensitive to the properties of the filler material used in the pole cut. This

question is addressed in the sensitivity analysis later in the report. Note that with G-10 material properties for the filler material, the distribution is quite similar to merely removing the symmetry boundary conditions for the pole without any filler material. (compare data in Table 4 and 5).

Fig. 7(b) shows the model used to analyze the option of using the vacuum pipe with epoxy in the pole cut. The radial thickness of the pipe considered in the analysis is 0.5 mm. Table 5 lists the stresses in the magnet at various stages. Note that the peak stress in the coils is reduced from 115 MPa to 96 MPa at Position - 1 with the addition of the vacuum pipe. However the stresses in the pipe itself are rather high; on the order of 700 MPa after cool down. Its quite likely that the vacuum pipe might deform plastically, which leads to large deformations. But the maximum shear stress at the pipe/coil interface is about 30 MPa, so the possibility of epoxy failure is less. Note that unless otherwise stated, the discussion for the rest of the report is with epoxy in the pole cut and without the vacuum pipe.

4.2 Orthotropic Material Properties for the Nb_3Sn Coil

In all the previous analysis, the material properties for the Nb_3Sn coil were considered to be isotropic with modulus same as that of the coil azimuthal modulus. This was partly due to insufficient data available on the mechanical properties of the coil. Recently we have finished the measurements of the thermo-mechanical properties of the Nb_3Sn ten-stack samples in all the three directions. The modulus in the radial direction was measured to be 44 GPa at 300 K and 55 GPa at 4.2 K. Note that in azimuthal direction the modulus is 38 GPa both at 300 K and at 4.2 K. Further the coefficient of thermal contraction in radial direction was measured to be 2.6 μm/mm from 293 to 4.2 K compared to 3.5 μm/mm along azimuthal direction. See FERMILAB-Conf-99/052 for more details.

In order to input the orthotropic material properties for the coil assembly in cylindrical coordinates, the elements in the ANSYS model had to be generated in local cylindrical coordinate system by issuing the following commands before meshing:

```
Local, 11, 1          !create a local cylindrical coordinate system
esys,11               !generate the elements in cylindrical coordinate system
```

We can then specify the thermo-mechanical properties along the radial direction as properties along x-direction and along azimuthal direction as properties along y-direction. For similar boundary conditions, the Table 7 lists the stresses in the coil assembly for isotropic and orthotropic material properties. Since the material properties of the coil along radial and azimuthal direction are similar at room temperature, the stress values in the coil are also comparable. However on cool down, the peak stress with orthotropic material properties is 130 MPa, whereas with isotropic material properties, it is 114 MPa. This is due to the fact that the modulus along radial direction jumps from 44 to 55 GPa where as the azimuthal modulus remains almost the same.

	Coil with Isotropic Properties Azimuthal Stress, MPa				Coil with Orthotropic Properties Azimuthal Stress, MPa			
	300 K	**4.2 K**	**11 T**	**12 T**	**300 K**	**4.2 K**	**11 T**	**12 T**
COIL								
Position 1	74	114	7	-11	75	130	13	0
Position 2	90	32	100	101	95	25	91	103
Position 3	63	95	65	60	65	83	58	51
Position 4	74	105	111	115	75	106	102	115

Table 7: *Comparison of the stresses in the coil with isotropic and orthotropic material properties [clamp/yoke interference = 0.4 mm; spacer/pole interference = 0.15 mm; weld shrinkage = 0.4 mm].*

To reduce the coil prestress, the yoke/clamp and spacer/pole interference were optimized. Tables 8 and 9 lists the stresses in the various components of the magnet for two possible boundary conditions. Table 8 shows the values with yoke/clamp interference of 0.325 mm and spacer/pole interference of 0.15 mm. Table 9 shows for 0.3 mm and 0.10 mm.

	Azimuthal Stress, MPa				Radial Stress, MPa			
	300 K	**4.2 K**	**11 T**	**12 T**	**300 K**	**4.2 K**	**11 T**	**12 T**
COIL								
Position 1	65	116	5	-11	1.3	0	0	0
Position 2	83	24	80	90	1.3	0	0	0
Position 3	56	70	48	40	33	70	60	50
Position 4	65	93	90	103	37	53	100	103
SPACER	200	166	166	140	44	67	90	95
σ_{coil}(max)	83	117	92	95	=Von-mises stress			
CLAMP	140	117	120	120	=Von-mises stress			
SKIN	202	330	338	340	=Von-mises stress			
δR	2	-94	-25	0	=R(mid-Plane)-R (pole); μm			

Table 8: *Stresses in the various components of the magnet with yoke/clamp interference of 0.325 mm and spacer/pole interference of 0.15 mm.*

	Azimuthal Stress, MPa			
	300 K	**4.2 K**	**11 T**	**12 T**
COIL				
Position 1	69	122	9	-5
Position 2	73	23	82	93
Position 3	60	85	51	44
Position 4	65	97	93	103

Table 9: *Stresses in the various components of the magnet with yoke/clamp interference of 0.3 mm and spacer/pole interference of 0.1 mm.*

The azimuthal stress distribution in the coil assembly for yoke/clamp interference of 0.325 mm and spacer/pole interference of 0.15 mm is shown in the Appendix.

4.3 Stress in the Coils Before and After Spring Back

The stress distribution in the coils before the spring back i.e., while inserting the clamps into the yoke gaps was computed by giving an arbitrarily very high modulus to the clamp material. Note that this analysis was carried out without the skin. Fig. 8(a) shows the azimuthal stress distribution in the coil assembly. The coil sees this distribution during compression of the yoke assembly by hydraulic press to insert the clamps. The peak stress is about 90 MPa.

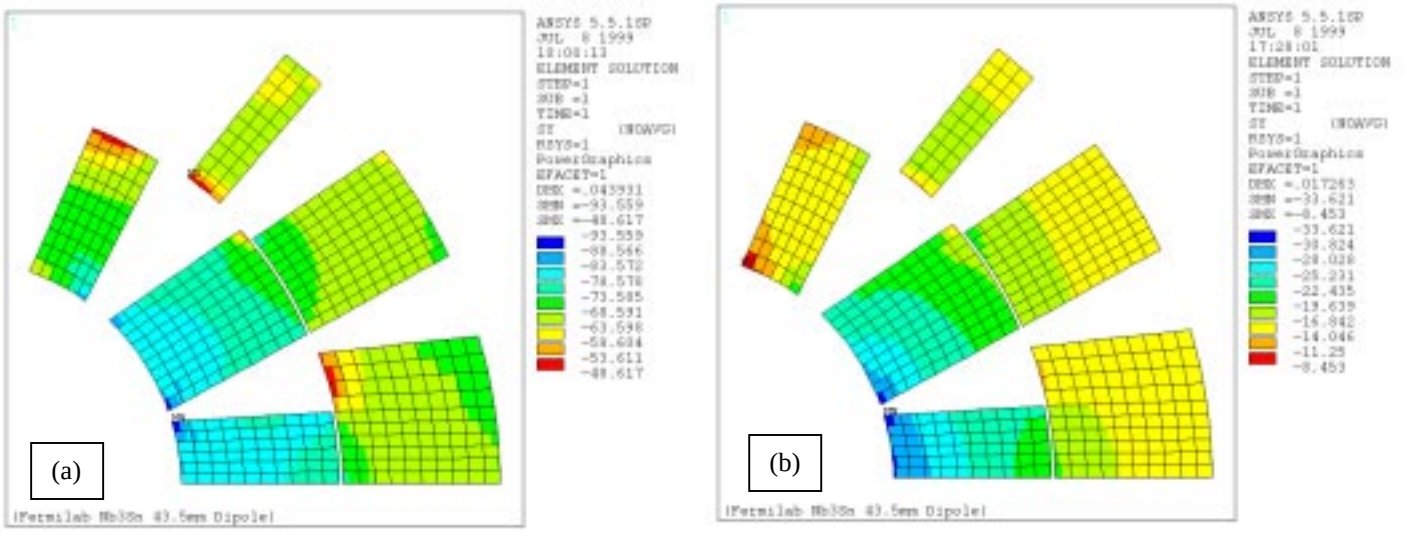

Figure 8: *Azimuthal stress distribution in the coil assembly (a) before spring back and (b) after spring back.*

Once the clamps are inserted and the hydraulic press is released, the coils spring back due to deformation in the clamp and yoke assembly thus decreasing the pre-stress. Fig. 8(b) shows the azimuthal stress distribution after spring back. The peak stress in the coils is only around 35 MPa. Note that in this case the clamp material was chosen as aluminum. The peak stress in the clamp with the slot for skin alignment key is about 200 MPa. The x-displacement of the clamp after the spring back is about 0.045 mm.

5.0 Sensitivity Analysis

The following effects are analyzed :

- Effect of deviation in the clamp length i.e., clamp/yoke interference
- Effect of deviation in spacer / pole interference
- Effect of deviation in the OD of the "pipe"
- Effect of variation in the weld shrinkage
- Effect of the stiffness of the filler material in the cut
- Effect of variation in the coefficient of thermal shrinkage of the Nb_3Sn coils

The first four will give us the effect of tolerances on the magnet performance. The last two will effect the peak stress in the coil assembly after cool down. It is essential to keep the peak stress below 125 MPa to reduce the degradation in the cable. The last variation was analyzed as the thermal contraction data available in the literature for Nb_3Sn coils has a large scatter and we should be positively sure that the coil assembly is under compression at 11 T. The criteria for acceptable tolerances are (i) The peak stress in the coils should be less than 125 MPa and (ii) the coils should be in compression at all stages of the magnet.

5.1 Effect of deviation in the Clamp/Yoke Interference

The clamp/yoke interference was varied from 0.25 to 0.45 mm with spacer/pole interference of 0.1 mm and weld shrinkage of 0.4 mm. Since the most critical in the coil assembly being the Position - 1, the Fig. 9 shows the variation of stress with clamp interference for this position. If the coil has be in compression at all stages of the magnet, the minimum clamp/yoke interference is 0.275 mm. However if the peak stress has to be less than 125 MPa, the maximum interference allowed is 0.375 mm. Hence the acceptable range is 0.275 to 0.375 mm.

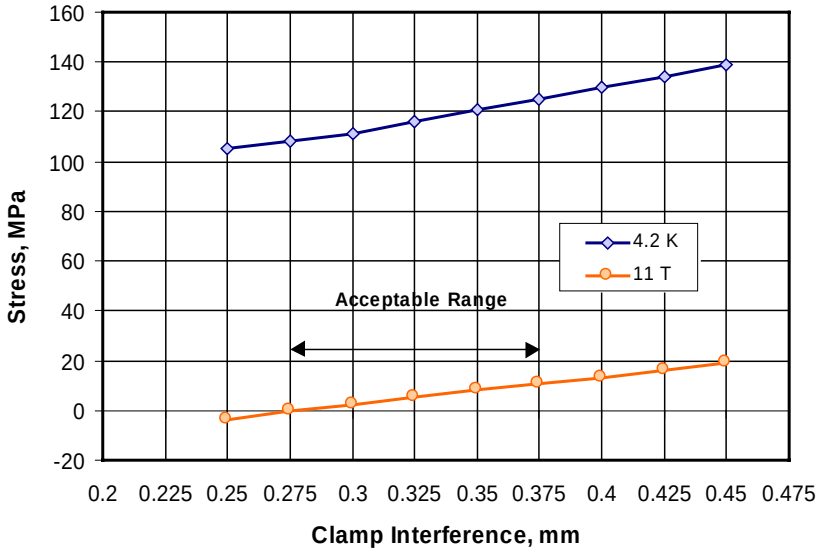

Figure 9: *Effect of deviation in clamp/yoke interference.*

5.2 Effect of deviation in the Spacer/Pole Interference

Fig. 10 shows the variation of the stress at Position - 2 with respect to the spacer/pole interference. The purpose of this interference is to avoid excessive stress in the coils at room temperature. The peak stress in the coil increases with the decrease in spacer/pole interference. The acceptable range is 0.1 to 0.175 mm with 0.30 mm clamp/yoke interference and 0.4 mm of weld shrinkage.

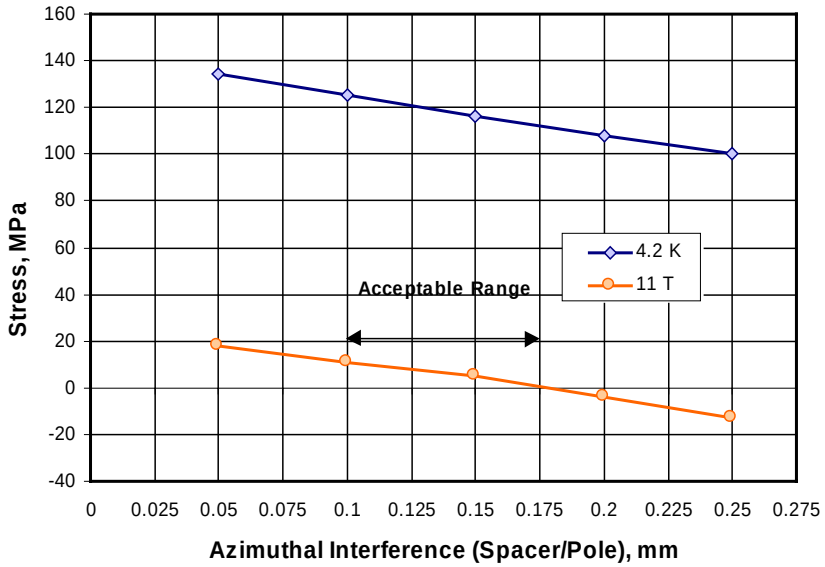

Figure 10: *Variation of the coil prestress at Position - 1 with spacer/pole interference.*

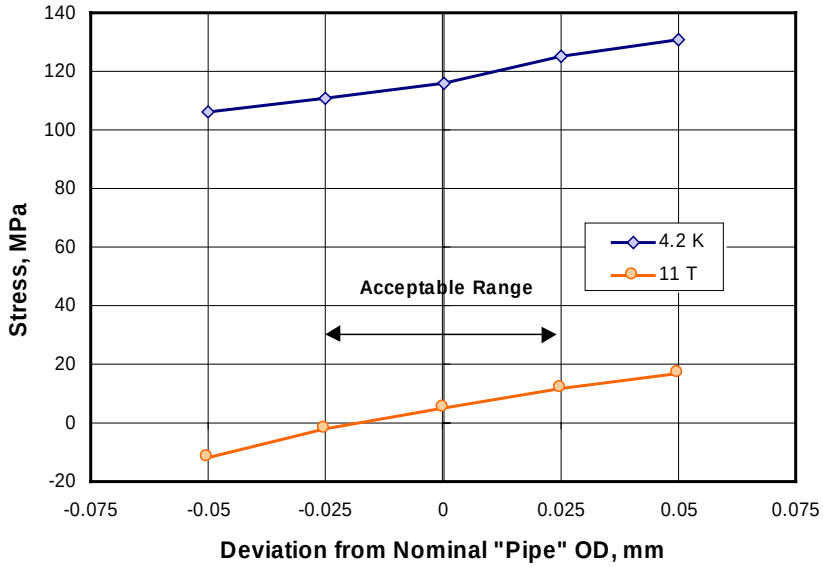

Figure 11: *Variation of the coil prestress at Position - 1 with deviation in "pipe" OD.*

5.3 Effect of deviation in "Pipe" OD

The deviation in the "pipe" OD was varied from -0.05 to +0.05 mm with clamp/yoke interference of 0.3 mm, spacer/pole interference of 0.1 mm and weld shrinkage = 0.4 mm. Fig. 11 shows the variation of stress with deviation in pipe OD. This is probably the most critical dimension, as the allowed variation is only -0.025 to +0.025 mm.

5.4 Effect of variation in the modulus of the filler material

The machined section in the pole will be filled with some material and then impregnated with epoxy. The goal is to check the effect of the stiffness of this material on the coil prestress. The clamp/yoke interference was taken as 0.3 mm, spacer/pole interference = 0.1 mm and weld shrinkage = 0.4 mm. Fig. 12 shows the variation of the pre-stress at Position - 1 with elastic modulus of the filler material. It is clear from the graph that the lower the modulus of the filler material the better it is.

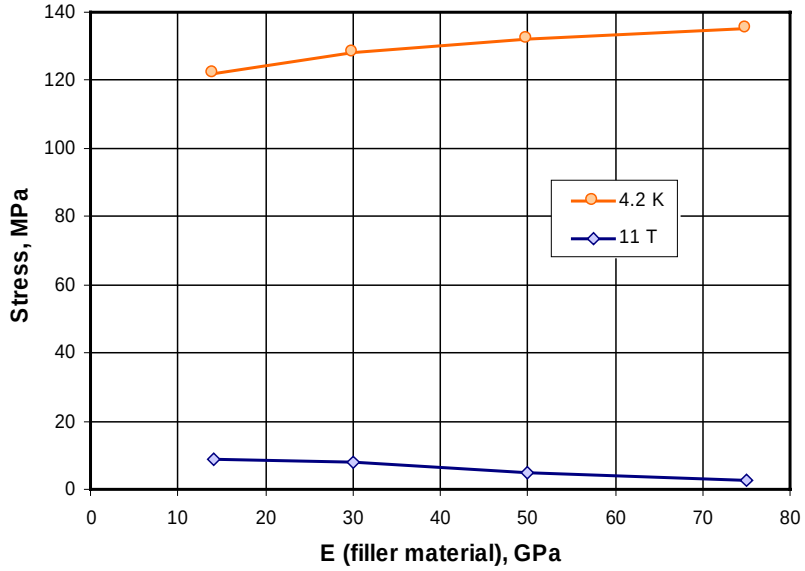

Figure 12: *Effect of variation in the elastic modulus of the filler material*.

5.5 Effect of variation in the Thermal Shrinkage of Nb_3Sn Coil Assembly

The thermal shrinkage of a epoxy impregnated Nb_3Sn composite was measured to be 3.5 mm/m from 293 K to 4.2 K. However there is a larger scatter in the literature and some concerns that the thermal contraction coefficient of the Nb_3Sn composite is larger than aluminum (~ 4.2 mm/m). To understand the effect of variation of thermal shrinkage on the magnet mechanics, analysis was carried out for various thermal shrinkage coefficients. Fig. 13 shows the results of these analysis. As the thermal contraction coefficient of the coil increases, the stress at Position - 1 decreases. Above 4 mm/mm, the coil sees tension at 11 T. These simulations were made with

clamp/yoke interference of 0.3 mm, spacer/pole interference of 0.1 mm and weld shrinkage of 0.4 mm.

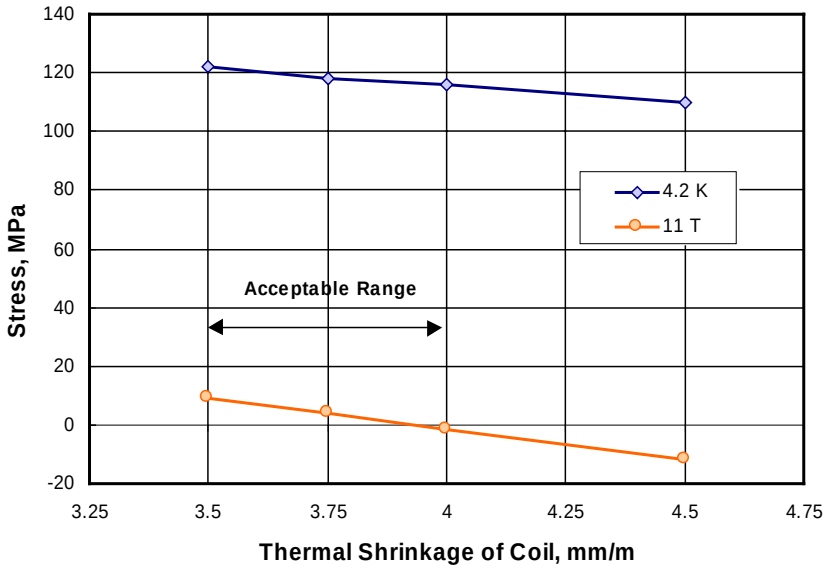

Figure 13: *Effect of variation of thermal shrinkage of coil assembly.*

Suppose that we would like to have the coil assembly under compression at 11 T for thermal contraction coefficient of 4.5 mm/m, then we have to increase the clamp/yoke interference to 0.35 mm (Fig. 14). However if we do this and the thermal contraction coefficient of the coil is actually 3.5 mm/m, then the peak stress in the coils would be 128 MPa.

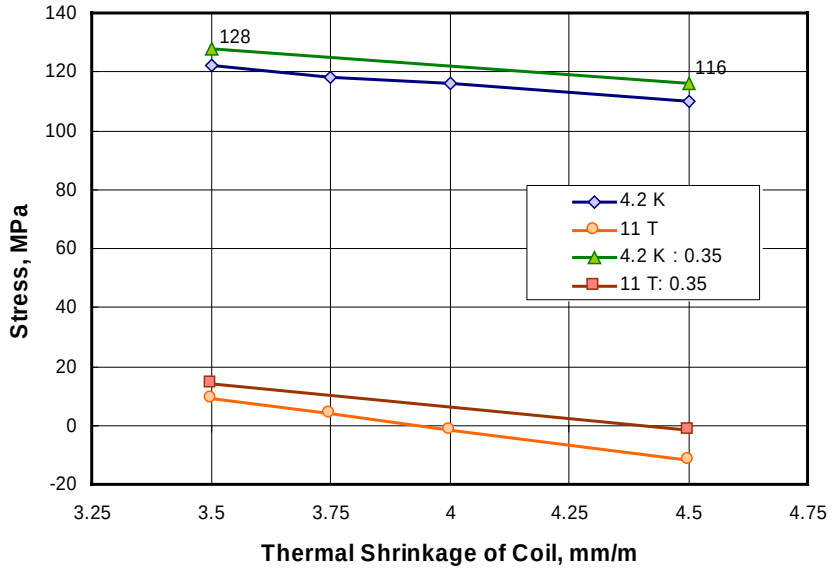

Figure 14: *Variation of pre-stress with thermal shrinkage of Nb_3Sn Composite.*

5.6 Effect of variation in the Weld Shrinkage

In the present design both the clamp and the skin act as structural elements. Thus the pre-stress to the coils is provided by the clamp/yoke interference and weld shrinkage. This section deals with the variation of weld shrinkage and how it effects the magnet mechanics. Fig. 15 shows the pre-stress at position - 1 for various weld shrinkage displacements. The clamp/yoke and spacer/pole interference were kept constant at 0.3 mm and 0.1 mm respectively. The pre-stress increases quite rapidly with weld shrinkage. The acceptable weld-shrinkage is between 0.3 to 0.45 mm.

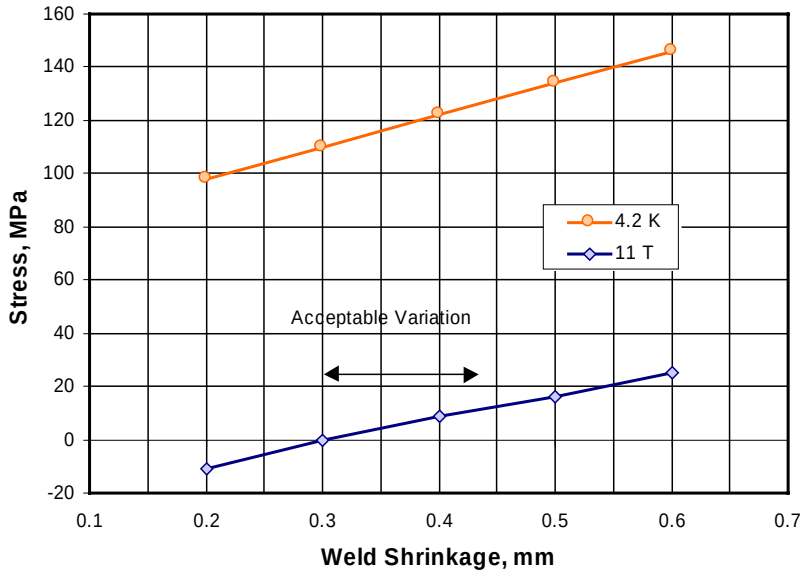

Figure 15: *Variation of Pre-stress with weld shrinkage.*

6.0 Summary

Mechanical and sensitivity analysis was performed for the 43.5 mm bore design. The optimum boundary conditions were determined and they are clamp/yoke = 0.325 to 0.3 mm; spacer/pole interference = 0.15 to 0.1 mm and weld shrinkage = 0.4 mm. Sensitivity analysis revealed that the yoke/clamp and spacer/pole interference can vary from 0.275 to 0.375 mm and 0.1 to 0.175 mm respectively. The "pipe" outer diameter has to be within 50 μm of the nominal design.

Azimuthal stress distribution with epoxy in the pole cut; no vacuum pipe

TD-99-035
07/16/99

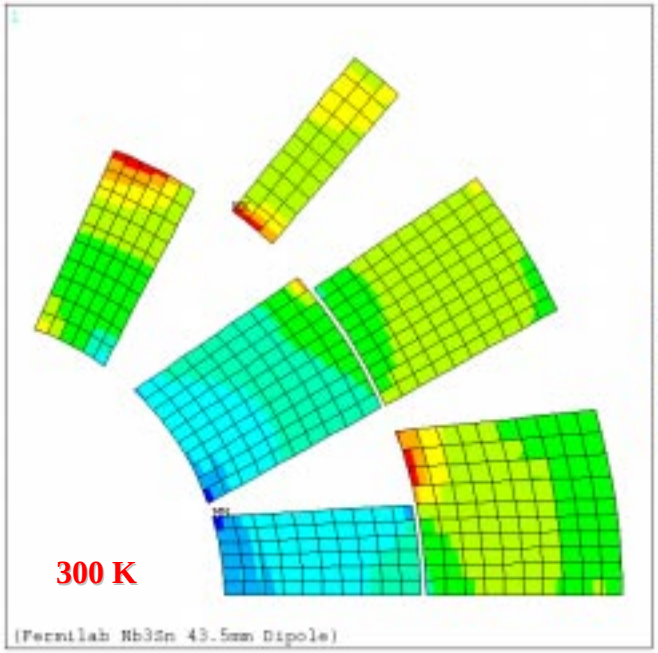

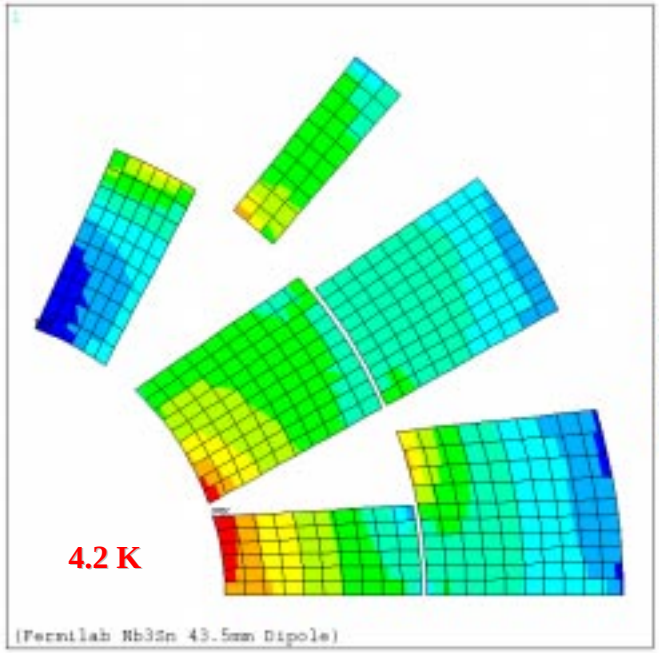

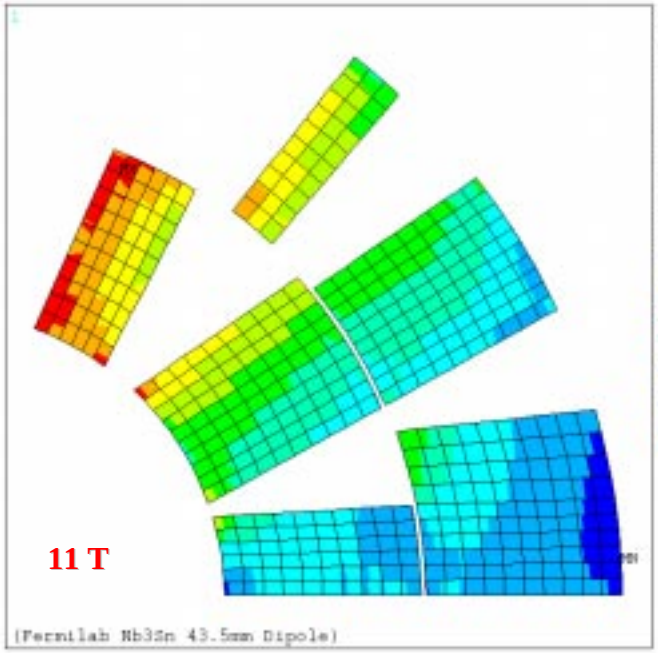

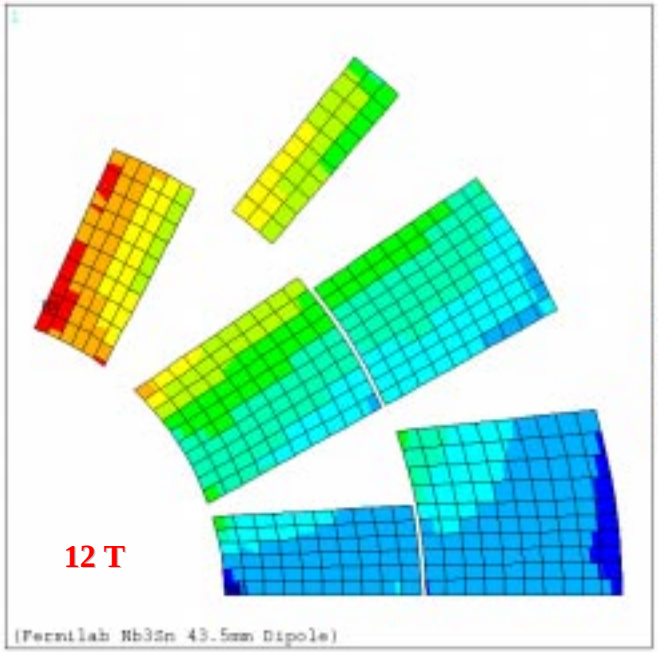

All units are in MPa

Azimuthal stress distribution with epoxy in the pole cut; with vacuum pipe

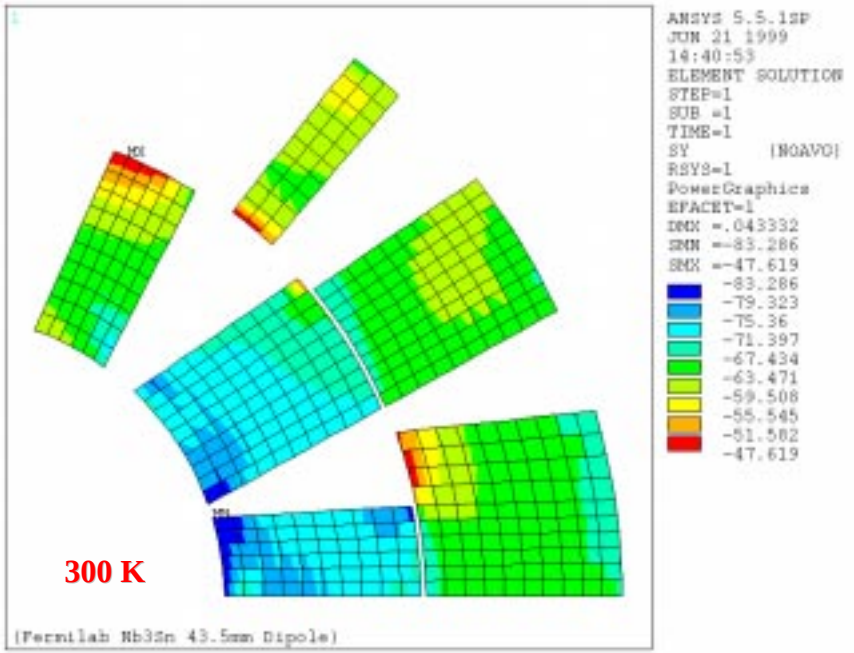

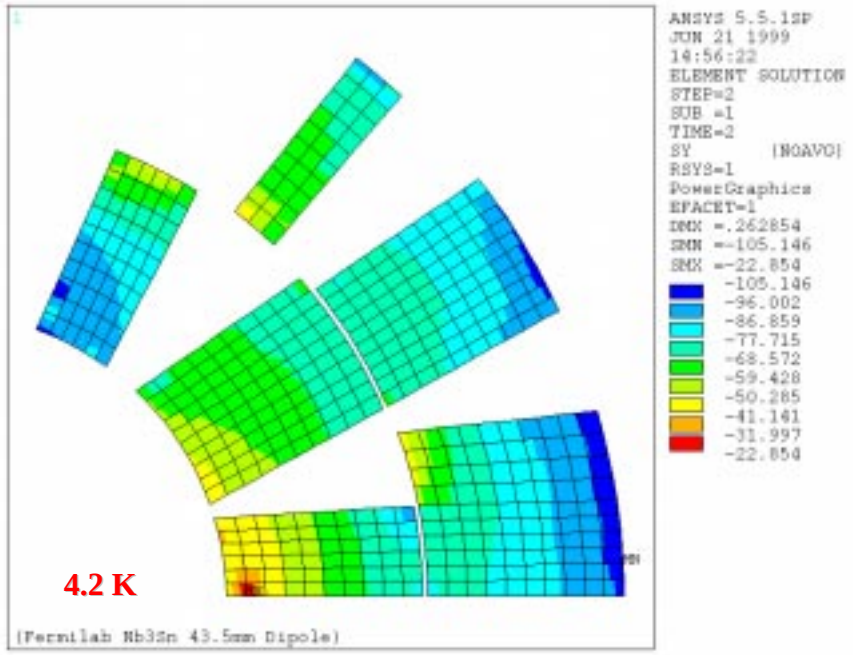

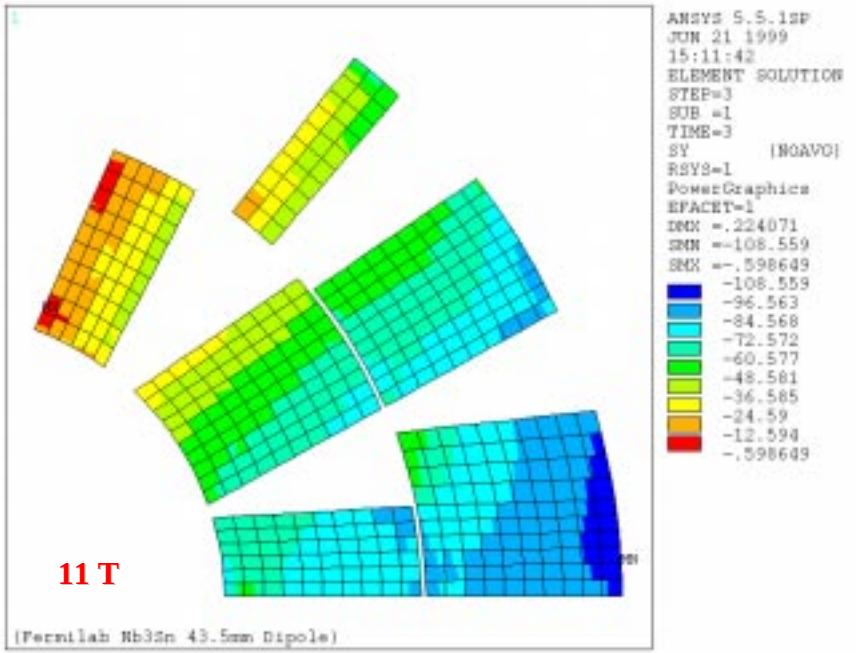

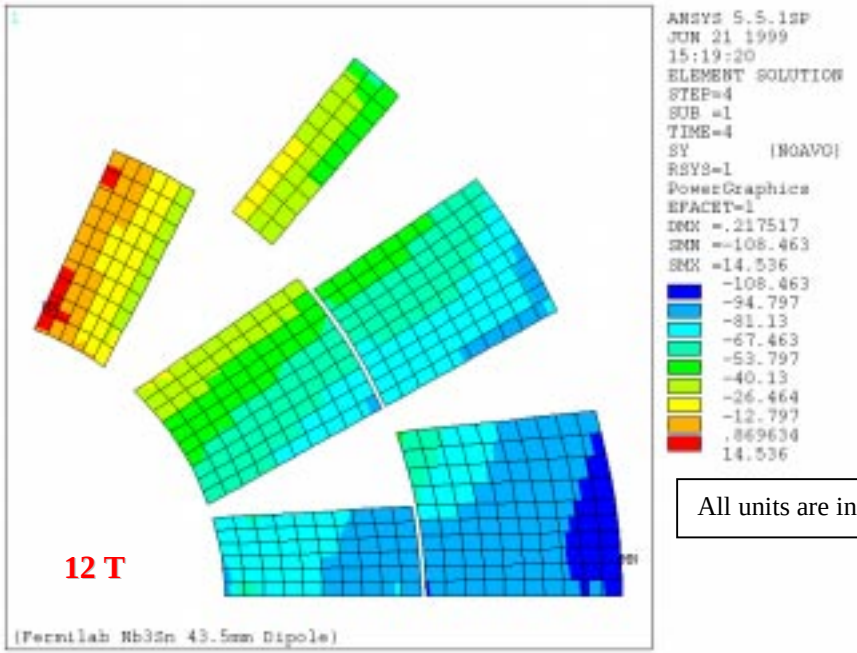

All units are in MPa

Azimuthal stress distribution with epoxy in the pole cut; no vacuum pipe; Conductor: Orthotropic